JOURNAL OF ENVIRONMENTAL GEOGRAPHY
Journal of Environmental Geography 6 (1–2), 1–8.
DOI: 10.2478/v10326-012-0001-5
ISSN: 2060-467X

CLASSIFICATION METHODS FOR INLAND EXCESS WATER MODELING

Boudewijn van Leeuwen[1*], László Henits[1], Minucsér Mészáros [2], Zalán Tobak[4], József Szatmári[1], Dragoslav Pavić[3], Stevan Savić[3], Dragan Dolinaj[3]

[1]Department of Physical Geography and Geoinformatics, University of Szeged, Egyetem u. 2-6, H-6722 Szeged, Hungary
[2]Center for Spatial Informations of Vojvodina, Faculty of Sciences, University of Novi Sad, Trg Dositeja Obradovića 3, 21000 Novi Sad, Serbia
[3]Climatology and Hydrology Research Centre, Faculty of Sciences, University of Novi Sad, Trg Dositeja Obradovića 3, 21000 Novi Sad, Serbia
*Corresponding author, e-mail: leeuwen@geo.u-szeged.hu

Research article, received 31 January 2013, published online 15 April 2013

Abstract

Inland excess water floodings are a common problem in the Carpathian Basin. Nearly every year large areas are covered by water due to lack of natural runoff of superfluous water. To study the development of this phenomenon it is necessary to determine where these inundations are occurring. This research evaluates different methods to classify inland excess water occurrences on a study area covering south-east Hungary and northern Serbia. The region is susceptible to this type of flooding due to its geographical circumstances. Three separate methods are used to determine their applicability to the problem. The methods use the same input data set but differ in approach and complexity. The input data set consists of a mosaic of RapidEye medium resolution satellite images. The results of the classifications show that all three methods can be applied to the problem and provide high quality satellite based inland excess water maps over a large area.

Keywords: classification, inland excess water, spectral mixture analysis, artificial neural network

INTRODUCTION

The year 2010 was one of the wettest years ever on the Carpathian Basin. In Szeged, almost twice as much precipitation fell as the long term yearly average (Van Leeuwen et al., 2012). This caused exceptionally large areas to be flooded by water. This phenomenon where water remains temporary in local depression because of a surplus of water due to lack of runoff, insufficient evaporation and low infiltration capacity of the soil or due to upwelling of ground water is called inland excess water. Factors that determine the sensitivity of an area to inland excess water are among others meteorology, relief, soil, groundwater, and human influences like land use and the construction of water works (Pálfai, 2004). Inland excess water damages crops, obstructs agricultural activities and local transportation, leads to soil and groundwater contamination and deterioration of the soil quality in the long term. In the border region of Hungary and Serbia, the natural circumstances are such that the area is vulnerable to inland excess water.

Different methods have been developed to determine the extent and location of inland excess water. Before the development of remote sensing techniques, the inundations could only be measured by observation in the field. This methods is expensive, time consuming and inaccurate. Visual interpretation of aerial photographs of inundated areas reduced the time needed to identify the floodings and reduced the inaccuracy but is expensive. This study uses (semi-) automatic classification methods to determine the occurrences of inland excess water based on satellite images. Provided that their resolution is high enough, satellite image classification can yield accurate results and is less expensive than traditional methods.

STUDY AREA

The study area is located in the cross border area between south-east Hungary and northern Serbia, covering 1600 km^2 in the wider surrounding of the towns of Szeged, Kanjiža and Novi Knezevac, extending on both sides of the Tisza River (*Fig. 1*). This relatively flat, and generally low lying territory (between 75 and 150 m) was formed predominantly by fluvial processes, as is illustrated by the abandoned meanders, natural levees, point-bar systems, scour channels and swales of the Maros and Tisza Rivers (Mezősi, 1983; Benyhe and

Kiss 2012), and also partly by eolian processes which shaped the higher geomorphologic units of loess terraces and sands (Bukurov, 1975; Davidović et al., 2003; Košćal et al., 2005).

Fig. 1 Overview map of the Hungarian – Serbian study area

Agriculture is one of the predominant economic activities, which also suffers the most damages due to the inundations. Inland excess water occurs frequently, mostly in low lying zones and also on higher geomorphologic units where local topographical, geological, hydrological and pedological conditions allow the formation of temporary standing surface water.

DATA AND METHODS

For this study, RapidEye satellite images were collected on March 24 and 25 of 2011, during the severe inland excess period of 2010-2011. The individual images were atmospherically corrected and mosaiced together covering an area of 5000 km^2. From the large mosaic, a sub image was created showing an area of about 40 x 40 kilometer (*Fig. 2*). Even after the atmospheric correction, several areas in the mosaic are severely affected by haze. This influences the quality of the classification results.

The RapidEye constellation, launched in 2008, is a system of 5 commercially operated satellites each carrying a 5-band multi-spectral imaging instrument providing daily revisiting time for every location between 84° N and 84° S on the Earth surface (RapidEye, 2012). The instrument acquires images in the spectral range between 440 and 850 nm (*Table 1*) with a spatial resolution of 6.5 meter (resampled to a pixel size of 5 meter) at nadir and a swath width of 77 kilometer. Due to the programmability of the satellites, they are more flexible than other satellites with global coverage like the Landsat satellites.

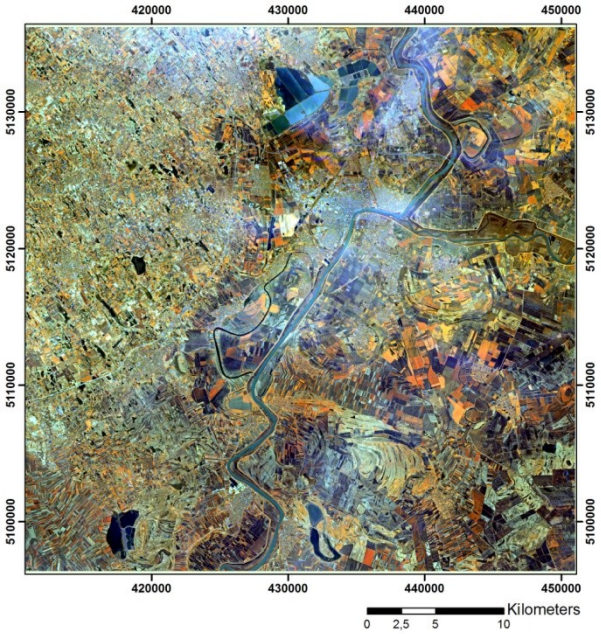

Fig. 2 RapidEye false color composite (bands 5-4-1) of the study area

Table 1 Spectral characteristics of RapidEye images

Band	Name	Spectral range (nm)
1	Blue	440 – 510
2	Green	520 – 590
3	Red	630 – 685
4	Red-Edge	690 – 730
5	Near Infrared	760 – 850

To investigate the best method to identify inland excess water based on remote sensing data, three classifications methods are executed on a RapidEye satellite image using the same training data set. The classification results were compared with areas defined in the training set.

Training data set

A training data set consisting of 8 classes (*Table 2*) was derived by delineating samples using a seed method, where starting from one clear pixel – adjacent, spectrally similar – pixels were selected. In this way, a minimum of spectrally mixed pixels is added to the training data set. Every class is represented by several thousands of pixels. Proper sampling of the intermediate classes like saturated soil and vegetation in water is difficult without fieldwork, and therefore these classes are not included. A "High albedo" class was added to the training class containing very bright pixels.

Table 2 Training classes

	Class name		Class name
1	Inland excess water	5	Vegetation3
2	High albedo	6	Deep water
3	Vegetation1	7	Bare soil
4	Vegetation2	8	Shallow water

Maximum Likelihood

The Maximum likelihood (ML) classification is a commonly used supervised classification technique, which directly uses all bands of the data set to define the statistical relationship between the input and output data. The maximum likelihood classification is a statistical approach where the probability of a pixel belonging to each of the predefined set of classes is calculated, and the pixel is then assigned to the class for which the probability is the highest (Tso and Mather, 2009). The method assumes a multivariate normal (Gaussian) distribution of the classes in the data set. This assumption of normality is generally reasonable for spectral response distributions in satellite imagery (Lillesand et al., 2004). The method is computational intensive because the probability for every class needs to be calculated.

Spectral Mixture Analyses

The aim of Spectral Mixture Analysis (SMA) is to determine the spatial ratio of spectrally homogeneous land cover types, the so-called endmembers, within a pixel. Each endmember specifies an unmixed, pure land cover type. The Linear Spectral Mixture Analysis (LSMA) is an improvement of the SMA method, by which the ratio of land cover types can be determined by using minimum two, and in case of a RapidEye image, maximum five endmembers. To be able to solve the linear system of equations (1), the number of the endmembers has to be less than or equal to the number of the spectral bands of the image.

$$R_b = \sum_{i=1}^{N} f_i \cdot R_{i,b} + \varepsilon_b \qquad (1)$$

R_b: the reflectance value of the image in band b;
N: the number of endmembers;
f_i: the ratio factor of endmember i;
R_{ib}: the reflectance value of the i^{th} endmember in band b;
ε_b: residual error.

The sum of the ratio factors of the endmembers equals 1 in every pixel and $f_i \geq 0$.

$$\sum_{k=1}^{n} f_{i,k} = 1 \qquad (2)$$

The suitability of the model can be determined on the basis of the ε_b residual error or on the basis of the value of the root mean square error (RMSE) for each band of the image.

$$RMSE = \frac{\sqrt{\sum_{i=1}^{n} \varepsilon_i^2}}{n} \qquad (3)$$

There are several techniques to select the endmembers. They can be selected from the different bands of the satellite images or 2 D scatter plots worked out from the bands (Rashed et al., 2001). By Principal Component Analysis (PCA), the endmembers are easier to determine, since it assembles almost 90% of the data variance into the first two or three bands and reduces the correlation between the bands to a minimum (Smith et al., 1985). Another frequently used method is to apply a transformation called the minimum noise fraction (MNF) method. This method consists of two main steps: (1) in the first step the noise fractions of the data set are decorrelated and rescaled on the basis of an estimated noise covariance matrix, resulting in transformed data, of which the noise has unit variance and where there is no correlation between the bands; (2) in the second step a traditional PCA is carried out (Green et al., 1988). In this research, the PCA method was used to determine the endmembers.

In the first step, PCA images were created for the RapidEye image taken on 24th March 2011, which resulted in another 5 bands. The information content of the images is continuously decreasing after one another, thus the first three bands contain 98.9% of the total information content. The last bands predominantly contain noise.

Based on the first three PCA images, three endmembers were defined for the linear spectral mixture: (1) the water surfaces, (2) the vegetation, and (3) the soil. These endmembers were pointed out in the spectral space formed by the first three PCA-bands and were detected at the margins and peaks of the 2D scatter plot. In the created fraction maps, for every single pixel the percentage of one of the three categories is calculated. A pixel value of 1 means that the pixel is homogenous and that it consists of 100% of the specific category. In the final step of the SMA methods, the newly generated 3 band endmember composite is used as input data for a maximum likelihood classification as described above. In the LM classification the same training data set was used as in the other two classification methods.

Artificial neural networks

Artificial neural networks (ANN) are computational models that mimic the functioning of the human brain. They are computational mechanisms that are able to acquire, represent, and compute a mapping from one multivariate space of information to another, given a set of data representing that mapping (Atkinson and Tatnall, 1997). Schematically, a basic artificial neural network can be presented as a structure consisting of multiple layers of interconnected nodes as shown in *Figure 3*.

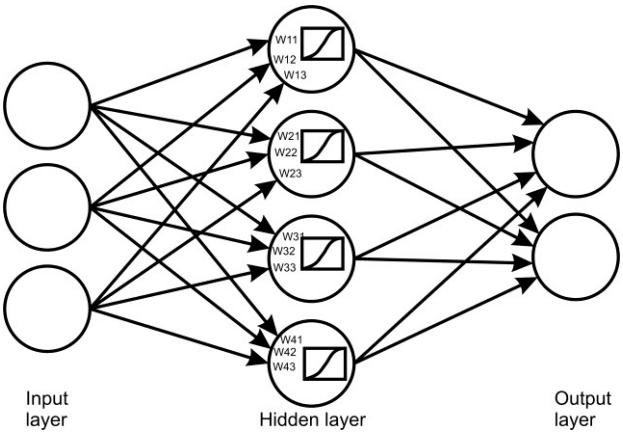

Fig. 3 Basic artificial neural network

Table 3 Cross table showing the training validation of the maximum likelihood classification

Training	ML result								Number of pixels	User Acc
	1	**2**	**3**	**4**	**5**	**6**	**7**	**8**		
1	2944	0	0	0	25	1096	0	8	4073	0.72
2	0	3542	0	0	0	0	67	0	3609	0.98
3	0	0	4568	9	0	0	0	0	4577	1.00
4	0	4	133	9774	112	0	3	0	10026	0.97
5	19	0	0	36	5408	0	0	2	5465	0.99
6	995	0	0	0	1	8968	0	0	9964	0.90
7	0	187	0	13	1	0	9489	0	9690	0.98
8	0	0	0	0	0	0	10	8929	8939	1.00
# of pixels	**3958**	**3733**	**4701**	**9832**	**5547**	**10064**	**9569**	**8939**	**56343**	
Prod. Acc.	0.74	0.95	0.97	0.99	0.97	0.89	0.99	1.00		**OA=0.95**

The application of ANNs consists of two phases. The first phase is called the training phase. During this phase the ANN is presented with an input and an associate output data set. The training is a process that aims to adapt the network internally in such a way that the calculated results from the network are as close as possible to the expected results. Iteratively, the internal weights are adapted based on the direction in which the error is moving. When the error is not decreasing anymore, the weights are fixed and the network is stored. Subsequently, the network is used in the simulation phase where the trained network is presented with a new input data set that is similar to the input data set of the training phase. If the network was trained properly and the new input data covers the same problem domain as during the training phase, accurate results can be obtained.

One of the most popular artificial neural models used in pattern classification, prediction and regression tasks is the multilayer perceptron (MLP) (Atkinson and Tatnall, 1997; Demuth et al., 2010; Pradhan et al., 2010). An MLP is the feed forward multilayer network where a signal propagates in a forward manner from one layer to the next layer and is modified by the associated weights of each connection (Pradhan et al., 2010). This means that there is neither direct, nor indirect influence from a given neuron to its own inputs. The network has an input layer, at least one hidden layer and an output layer.

In an MLP, the signal of all input neurons is weighted and summed to a net output. This net output is then evaluated by an activation function where it produces an output. Different activation functions exist but with MLPs usually – and also in this study – log-sigmoid functions are used, which ensure non-linearity to the method.

MLPs are often combined with a backpropagation learning algorithm. The algorithm randomly selects the initial weights for every neuron and then calculates an output based on a set of inputs. The calculated outputs are compared to the expected output and the error is calculated. Subsequently, the weights are adapted based on the errors in such a way that the total error is distributed among the neurons in the network (Yang and Rosenbaum, 2001). To be able to calculate the effect of the change of the individual weights the first derivative of the activation function is needed. This requires that the activation function is differentiable. The process of feeding forward signals and back-propagating the errors via the output layer to the hidden layer is repeated iteratively until some targeted minimal error is achieved between the desired and actual output values of the network (Dawson and Wilby, 2001; Pijanowski et al., 2002, Pradhan et al., 2010). The weights are then stored to retain the knowledge in the network. After training, when presented with an arbitrary input pattern that is noisy or incomplete, the neurons in the hidden layers of the network will respond with an active output, if the new input contains a pattern that resembles the feature the individual neurons learned to recognize during the training (Hagan et al., 1996; Freeman and Skapura, 1991).

To calculated the inland excess water results in this study, a GIS - ANN framework (Van Leeuwen et al., 2012) was used, that is based on ArcGIS, a geographic information system and Matlab, a mathematical modeling software.

RESULTS

Validation is not possible based on ground truth data because it is not possible to collect inland excess water information from such a large area. Therefore internal validation is executed based on the training areas. This means that the results of the classifications are compared with the predefined training sets. In the case of the maximum likelihood and spectral mixture analysis all pixels from the input training set were used to perform the classification, while in case of the artificial neural network classification 70% of the training data was used for actual training and the other 30% was used for testing and validation of the training.

Maximum likelihood

The maximum likelihood classification has an overall accuracy of 0.95 (*Table 3*). The most problematic class is the Inland excess water (1) class with a user accuracy of 0.72. Many pixels are classified as Deep water (6). Obviously when combining these classes and the Shallow water (8) class as well, the results are much better. In this case, both the user and producer accuracy for the combined water class is 0.99. All other classes show very little misclassification.
Visual inspection of the output map reveals large areas covered with water in the east and south east (*Fig. 4*). The large lake systems in the north and along the Tisza River are properly classified. The areas with High albedo (2) are found in the city of Szeged, on the sand soils in the north-west, and in the south center.

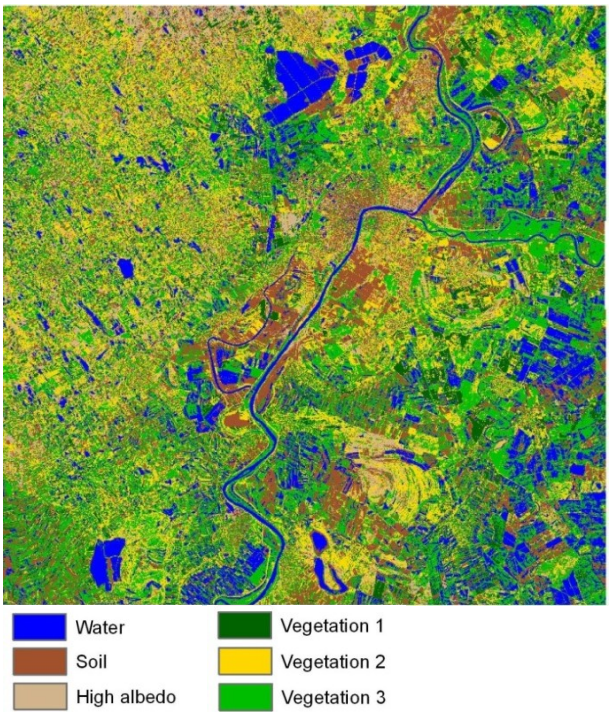

Fig. 4 Maximum likelihood classification result

Spectral mixture analysis

The overall accuracy of the SMA classification was 0.75 (Table 4). The accuracy of the Inland excess water (1) and Shallow water classes (8) are about 0.80 though. The Deep water class (6) is often misclassified as Soil (7). The reflectance of water is influenced by many factors, like suspended solids, water depth, bottom sediments, turbidity and color (Moore, 1980). These may cause classification errors. These errors are already appearing in the fraction images (*Fig. 5*). During this processing step, the high soil fraction in the lakes and the Tisza River is clearly visible.

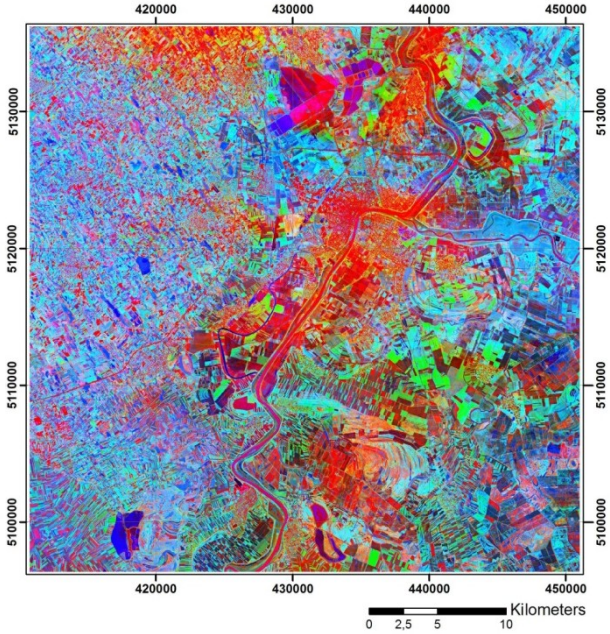

Fig. 5 Color composite of the three fraction maps (Red: soil, Green: vegetation, Blue: water)

The user accuracy of the High albedo class (2) is low due to extreme misclassification of the pixels as Bare soil (7) *(Table 4*). This is happening in areas with sandy soils, which have a very high reflectance.

On the thematic map resulting from the ML classification of the spectral mixture analysis result, it can

Table 4 Cross table showing the training validation of the spectral mixture analysis classification

Training	**SMA result**								**Number of pixels**	**User Acc.**
	1	**2**	**3**	**4**	**5**	**6**	**7**	**8**		
1	3318	0	0	0	26	729	0	0	4073	0.81
2	0	75	0	0	0	0	3534	0	3609	0.02
3	0	0	4577	0	0	0	0	0	4577	1.00
4	0	0	153	9783	90	0	0	0	10026	0.98
5	5	0	0	74	5386	0	0	0	5465	0.99
6	1816	0	0	0	1	8147	0	0	9964	0.82
7	0	0	0	0	1	0	9689	0	9690	1.00
8	3	0	0	0	0	0	7519	1417	8939	0.16
# of pixels	**5142**	**75**	**4730**	**9857**	**5504**	**8876**	**20742**	**1417**	**56343**	
Prod. Acc.	0.65	1.00	0.97	0.99	0.98	0.92	0.47	1.00	0.65	**OA= 0.75**

be seen that Deep water (6) is sometimes misclassified as Soil (6) (*Fig. 6*). The large lake in the North (Fehér tó) and the Tisza River are assigned to the Soil class. The classification results of the Inland excess water class (1) are similar for all three classification methods. The High albedo class (2) is occuring the least often. This class is only found in smaller patches in the north west of the thematic map.

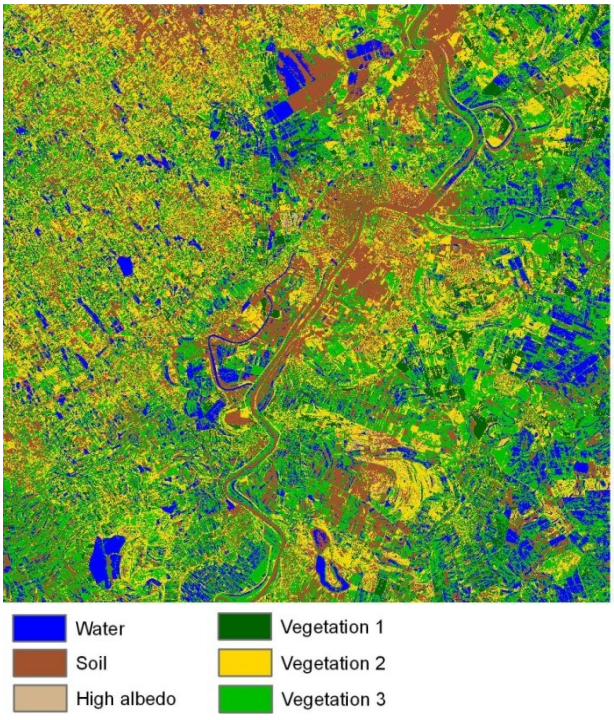

Fig.6 Spectral mapping analysis result

Artificial neural network

The classification using an artificial neural network also mixes the different water classes (1, 6, 8) (*Table 5*). Combining these classes into one bigger class increases the producer accuracy from 0.84 to 0.99 and the user accuracy from 0.68 to 0.99. Other misclassification only rarely happen resulting in an overall classification of 0.96.

The thematic map showing the classification result of the ANN method (*Fig. 7*) is similar to the ML result, although more areas are classified as High albedo (2) and less as Soil (7). Like with the SMA method, a part of the Fehér tó is misclassified as Soil. The Vegetation 3 class (5) is less common in this result compared to the other two methods, while the Vegetation 2 class (4) can be found more frequently.

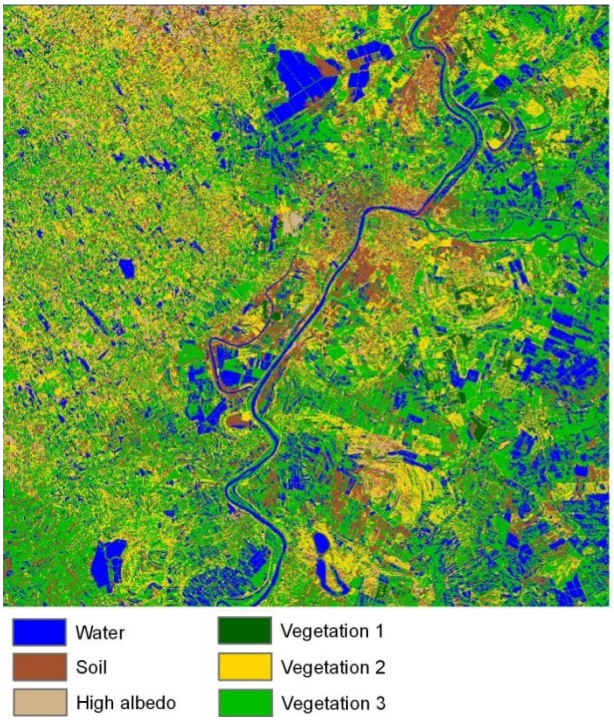

Fig. 7 Artificial neural network classification result

Comparison

All three classification methods result in a map showing areas where inland excess water was occurring during the acquisition of the images. Visually, the results seem quite similar, but the statistical comparison shows large differences (*Tables 4-6*). The SMA classification shows the lowest overall accuracy, but this is mainly due to the misclassification of one class. The ML and ANN meth-

Table 5 Cross table showing the training validation of the artificial neural network classification

Training	**ANN result**								**Number of pixels**	**User Acc**
	1	**2**	**3**	**4**	**5**	**6**	**7**	**8**		
1	2754	0	0	0	18	1297	0	4	4073	0.68
2	0	3542	0	0	0	0	67	0	3609	0.98
3	0	0	4565	12	0	0	0	0	4577	1.00
4	0	0	10	9965	42	0	9	0	10026	0.99
5	25	0	0	61	5377	1	0	1	5465	0.98
6	508	0	0	0	1	9455	0	0	9964	0.05
7	0	54	0	3	3	0	9630	0	9690	0.99
8	0	0	0	0	0	0	3	8936	8939	1.00
# of pixels	**3287**	**3596**	**4575**	**10041**	**5441**	**10753**	**9709**	**8941**	**56343**	
Prod. Acc.	0.84	0.98	1.00	0.99	0.99	0.88	0.99	1.00		**OA=0.96**

ods have similar overall accuracies. The Maximum Likelihood classification method is relatively simple and requires the least user input.

The overall accuracy is based on the principal diagonal of the confusion matrix only, and thus does not use the information from the whole confusion matrix. The Kappa coefficient (Cohen, 1960) though provides a measure of agreement between predicted values and the observed values while using all information in the confusion matrix (Tso and Mather 2009). Its value is always less than or equal to 1. A value of 1 implies perfect agreement and values less than 1 imply less than perfect agreement. Table 5 shows the Kappa and overall accuracy values for the three classifications.

Table 6 Accuracy measurements of the three classification methods

	Overall accuracy	**Cohen's Kappa**
Maximum Likelihood	0.95	0.94
Spectral mixture analysis	0.75	0.71
Artificial neural network	0.96	0.96

Also the amount and type of water differs per methods (*Fig. 8*). Most pixels are classified as Inland excess water with the SMA method, while with this method the Shallow water class is identified far less frequently. The inland excess water pixels are probably classified as shallow water by the other methods.

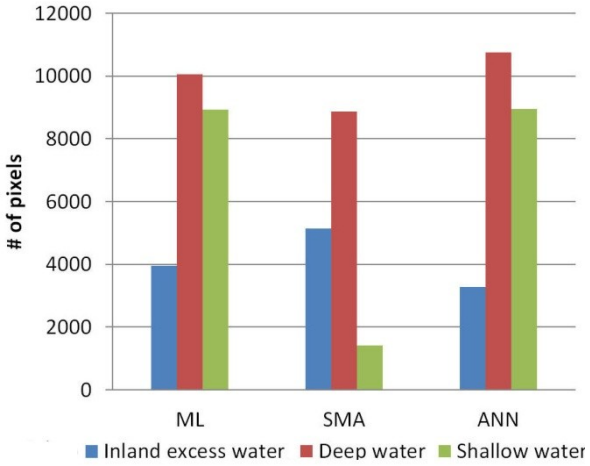

Fig. 8 Distribution of water classes per classification method

CONCLUSION

All three methods can be applied to classify inland excess water successfully and provide high quality maps of the inundations based on satellite data from a large area. There are difficulties for all methods though to distinguish between different type of water classes. The overall accuracy and Kappa coefficient of all classifications is high, but large individual differences exist. The images of the RapidEye satellite constellation have a high temporal coverage, large spatial coverage and acceptable spatial resolution. This makes them very suitable for inland excess water studies.

Acknowledgement

This research has been financially supported by the IPA Cross-border cooperation Programme of the European Union under the project titled MERIEXWA "MEasurement, monitoring, management and RIsk assessment of inland EXcess WAter (Using remotely sensed data and spatial data infrastructure)" HUSRB/1002/121/088.

References

Atkinson, P.M., Tatnall, A.R.L. 1997. Introduction neural networks in remote sensing. *International Journal of Remote Sensing* 18, 699–709.

Benyhe, B., Kiss, T. 2012. Morphometric analysis of agricultural landforms in lowland ploughed fields using high resolution digital elevation models, *Carpathian Journal of Earth and Environmental sciences* 7 (3), 71–78.

Bukurov, B. 1975. Fizičko-geografski problemi Bačke. SANU, Odeljenje prirodno-matematičkih nauka, Posebna izdanja 43 (Physical geographic problems of Backa. Serbian Academy of Sciences and Arts, Natural Sciences Section, Special editions 43), Belgrade, 209 p.

Cohen, J. 1960. A coefficient of agreement for nominal scale. *Educational and Psychological Measurement* 20, 37–46.

Davidović, R., Miljković Lj., Ristanović B. 2003. Reljef Banata. Univerzitet u Novom Sadu, Prirodno-matematički fakultet, Departman za geografiju, turizam i hotelijerstvo, Novi Sad (Relief of the Banat. University of Novi Sad, Faculty of Science, Department of Geography, Tourism and Hotel management), Novi Sad, 188 p

Dawson, C.W., Wilby, R.L. 2001. Hydrological modelling using artificial neural networks. *Progress in Physical Geography* 25 (1), 80–108.

Demuth, H., Beale, M., Hagan, M. 2010. Neural Network Toolbox 6. User's Guide. The Mathworks, 901 p.

Freeman, J.A., Skapura, D.M. 1991. Neural Networks: Algorithms, Applications and Programming Techniques. Addison-Wesley, Reading (MA), 550 p.

Green, A.A., Berman, M., Switzer, P., Craig, M.D. 1988. A transformation for ordering multispectral data in terms of image quality with implications for noise removal. *IEEE Transactions on Geoscience and Remote Sensing* 26, 65–74.

Hagan, M.T., Demuth, H.B., Beale, M.H. 1996. Neural Network Design. Boston, MA., PWS Publishing, 734 p.

Lillesand, T.M., Kiefer, R.W., Chipman, J.W. 2004. Remote Sensing and Image Interpretation. Wiley, 784 p.

Košćal, M., Menković, Lj., Mijatović, M., Knežević, M. 2005. Geomorfološka karta AP Vojvodine 1:200.000. Geozavod-Gemini Beograd. (Geomorphologic map of the Vojvodina Autonomous province 1:200000. Geoinstitute-Gemini, Belgrade)

Mezősi, G. 1983. Szeged geomorfológiai vázlata (Geomorphological features of Szeged). *Alföldi Tanulmányok* 7, 59-75. (in Hungarian)

Moore, G.K. 1980. Satellite remote sensing of water turbidity. *Hydrological Sciences-Bulletin-des Hydrologiques* 25 (4), 407–421.

Pálfai, I. 2004. Belvízek és Aszályok Magyarországon (Inland excess water and drought in Hungary). Hidrológiai tanulmányok, Budapest, 492 p. (In Hungarian)

Pijanowski, B.C., Brown, D.G., Shellito, B.A., Manik, G.A. 2002. Using neural networks and GIS to forecast land use

changes: a Land Transformation Model, Computers, *Environment and Urban Systems* 26, 553–575.

Pradhan, B., Lee, S., Buchroithner, M.F. 2010. A GIS-based back-propagation neural network model and its cross-application and validation for landslide susceptibility analyses, *Computers, Environment and Urban Systems* 34 (3), 216–235.

Rashed, T., Weeks, J.R., Gallada, M.S. 2001. Revealing the anatomy of cities through spectral mixture analysis of multispectral satellite imagery: a case study of the greater Cairo region, Egypt. *Geocarto International* 16 (4), 5–15.

RapidEye 2012. RapidEye Standard Image Product Specification, Version 3.0, Germany, www.rapideye.de [Last accessed: January 2013].

Smith, M.O., Johnson, P.E., Adams, J.B. 1985. Quantitative determination of mineral types and abundances from reflectance spectra using principal component analysis. *Journal of Geophysical Research* 90, 792– 804.

Tso, B., Mather, P. 2009. Classification Methods for Remotely Sensed Data, Second Edition. CRC Press, 376 p.

van Leeuwen, B., Mezősi, G., Tobak, Z., Szatmári, J., Barta, K. 2012. Identification of inland excess water floodings using an artificial neural network. *Carpathian Journal of Earth and Environmental sciences* 7 (4), 173–180.

Yang, Y., Rosenbaum, M.S. 2001. Artificial networks linked to GIS for determining sedimentology in harbours. *Journal of Petroleum Science and Engineering* 29, 213–220.